Excitation Process of Helium Atoms by the Impact of 100—200 keV Protons

By

Akio ITOH*, Masatoshi ASARI* and Fumio FUKUZAWA*

(Recieved March 25, 1977)

Abstract

Excitation cross sections of some states of helium by the impact of 100–200 keV protons were studied under various excitation conditions. The lateral distributions of light source were also measured. In the higher target gas pressure region, the excitation of $n^1P(n=3,4)$ levels are greatly increased by the effect of the imprisonment of resonance radiations, and the $4^{1,3}D$ and 3^3P levels are also influenced by the effect of a collisional transfer. The 4^1S state is mainly excited by a direct collision with incident protons even at the higher gas pressure.

1. Introduction

The study of processes leading to the formation of excited atoms as the results of ion-atom bombardment is of great fundamental interest. Information obtained by measuring light intensities of spectra emitted from the excited atoms under conditions of various projectile energies and target gas pressure are directly related to the excitation mechanism.

Many measurements of excitation of helium by the impact of protons have been reported[1-7]. Most of these studies were concerned mainly with the direct excitation process, and experiments have been made at very low target gas pressure where contributions of secondary excitation processes are negligible. However, it is necessary to consider both the direct and the secondary excitation processes to obtain the over-all features of the collision processes in the gas media. In the present study, therefore, we made the measurement over a wide range of target gas pressure.

Important secondary excitation mechanisms are as follows:

I) Imprisonment of resonance radiation, which must be taken into account for the state connected optically with the ground state,

II) Collisional transfer of an excited atom at one state to another excited state

* Department of Nuclear Engineering

under the gas kinetic region,

III) Secondary particle collisions.

Systematic studies on these secondary processes, however, have not been made in the case of the proton impact experiment. From this point of view, excitations of states 3^1P, 4^1S, 4^1P, 4^1D, 3^3P and 4^3D of helium were studied under various conditions. Furthermore, the light intensities as a function of the distance from the beam axis (lateral distribution) were measured in order to estimate the effect of imprisonment, because radiation from the region outside the beam axis may be expected in this case.

2. Experimental procedure

The experimental apparatus is the same as that described in the previous

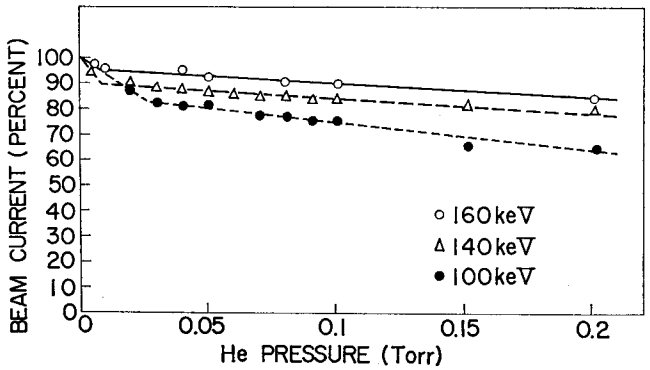

Fig. 1. The pressure and energy dependence of the proton beam current on a Faraday cup as a function of He gas pressure.

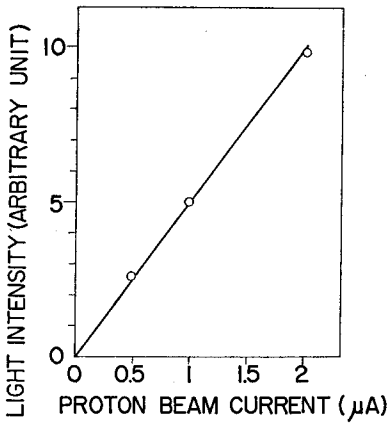

Fig. 2. Light intensity of 5016 Å produced by 145 keV proton impact on He at 1×10^{-1} Torr.

paper[8]. The incident proton energy was 100–200 keV and the beam current on a Faraday cup was about 0.5 μA. The gas pressure in the collision chamber varied from 1×10^{-4} to 1×10^{-1} Torr (background pressure was about 2×10^{-6} Torr). The beam current on the Faraday cup decreased as the gas pressure increased even at a constant incident beam flux as shown in Fig. 1. From these curves the correct incident proton current is easily obtained. It is interesting to note that the decrease of the Faraday cup current with an increase of gas pressure is slower for helium gas than that for nitrogen gas, which was shown in the previous paper. The proportionality of light intensity to the incident beam current was confirmed for some representative lines. An example of the 5016 Å line measured at a pressure of 1×10^{-1} Torr and at an energy of 145 keV is shown in Fig. 2. This proportionality measns that the effect of successive excitation of the target atoms is negligible[8].

3. Method of analysis

In this section, the relation between the number of helium atoms in some excited state produced by the proton impact, and the number of photons emitted spontaneously in the collision chamber is briefly described. Notations used in this paper have the following meanings.

ρ ; number density of target atoms per unit volume
ϕ ; number of incident protons per unit area per unit time
N_j ; number density of helium atoms in the excited state j
Q_j ; direct excitation cross section of helium from the ground state to state j by the proton impact
A_{ji} ; radiative transition probability from state j to state i
A_{j0} ; radiative transition probability from state j to the ground state
A_j ; sum of all radiative transition probabilities from the state j
A_j' ; sum of transition probability other than the A_{j0}
f_j ; the fraction of resonance radiations which are absorbed in the collision chamber
g_j ; imprisonment factor, $(1-f_j)$. That is, the fraction of the resonance radiation which escapes from the collision chamber
Q_{ki}^c ; collisional transfer cross section from state k to state i
v ; thermal velocity of target atom

When there are no secondary excitation processes, the rate of excitation of state j can be written as

$$\frac{d}{dt}N_j = \rho\phi Q_j - N_j A_j . \tag{1}$$

Under the condition where an equilibrium has been established between population and depopulation the number density of an excited state j is geven by

$$N_j = \frac{\rho\phi Q_j}{A_j} . \tag{2}$$

Also Eq. (2) can be rewritten as

$$Q_j = \frac{A_j N_j}{\rho\phi} . \tag{3}$$

In actual cases, there are always some secondary processes, and N_j depends complicatedly on the gas pressure. In these cases, a quantity corresponding to the excitation cross section is also defined as

$$Q_j' = \frac{A_j N_j}{\rho\phi} , \tag{4}$$

which is called an apparent excitation cross section.

The forms of Q_j' for some typical cases are described in the following.

I) Effect of imprisonemnt of resonance radiation

The transition probability from n^1P to the ground state 1^1S is very large because it is an optically allowed transition. A light emitted in this transition (resonance radiation) is easily absorbed by the surrounding target atoms in the ground state. In this case the rate equation of n^1P is written as;

$$\frac{d}{dt}N_j = \rho\phi Q_j - N_j A_j + N_j A_{j0} f_j = \rho\phi Q_j - (A_j' + A_{j0} g_j) N_j . \tag{5}$$

In equilibrium,

$$N_j = \frac{\rho\phi}{A_j' + A_{j0} g_j} Q_j . \tag{6}$$

The apparent excitation cross section, therefore, is given by

$$Q_j' = \frac{A_j}{A_j' + A_{j0} g_j} Q_j . \tag{7}$$

The imprisonment factor g_j depends both on the shape and the size of the collision chamber. For the determination of the shape, an independent effective chamber radius (the curves of $g_j(r)$ given by Gabriel and Heddle[9]) was used, which is

reproduced in Fig. 3.

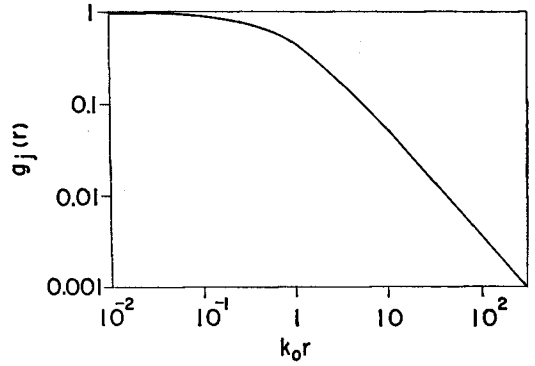

Fig. 3. Imprisonment factors for a resonance radiation. K_0 is the absorption coefficient at the peak of the line. (Reproduced from ref. 9).

II) Effect of collisional transfer

The transfer of excitation by collision with other target atoms is called collisional transfer. The reaction for such a transfer of excitation energy may be exemplified by the following:

$$\mathrm{He}(n^1P)+\mathrm{He}(1^1S) \rightarrow \mathrm{He}(n^{1,3}D)+\mathrm{He}(1^1S) .$$

In this case the rate equation is

$$\frac{d}{dt}N_j = \rho\phi Q_j - N_j A_j + \sum_k N_k \rho v Q^c_{kj} . \tag{8}$$

State k, in which the energy is close to that of state j, contributes to this process because only thermal kinetic energies are available to induce the process. Therefore, it is sufficient to take into account state k which has same principal quantum number as that of state j.

In equilibrium,

$$N_j = \frac{1}{A_j}[\rho\phi Q_j + N_k \rho v Q^c_{kj}] , \tag{9}$$

and the apparent excitation cross section is given by

$$Q_j' = Q_j + \frac{N_k}{\rho\phi}\rho v Q^c_{kj} . \tag{10}$$

By using the apparent excitation cross section Q_k' for state k, Eq. (10) is rewritten as

$$Q_j' = Q_j + Q_k' \tau_k \rho v Q^c_{kj} , \tag{11}$$

where τ_k is the life time of state k.

III) Effect of secondary particles

When protons pass through the gas, secondary particles such as neutral hydrogen atoms and electrons are produced as the results of charge changing collisions and ionization processes respectively. These secondary particles may excite the target atoms. The production rate of the excited state by this process may be written as

$$\frac{d}{dt}N_j = \rho\phi Q_j - N_j A_j + C_j\rho^2\phi\,, \tag{12}$$

where C_j is a constant which depends on the projectile energy, and is usually called a second-order coefficient. In equlibrium,

$$N_j = \frac{\rho\phi}{A_j}[Q_j + C_j\rho]\,, \tag{13}$$

and the apparent excitation cross section of the siate j is given by

$$Q_j' = Q_j + C_j\rho\,. \tag{14}$$

If observation of the transition is made by the detection of the corresponding light quanta, the photon counting rate R_λ is written as,

$$R_\lambda = F(\lambda)\int_V G(\lambda, \vec{x})\, J_{ji}(\vec{x})\, d^3\vec{x}\,, \tag{15}$$

where λ is the wave length of light emitted in the transition $j \to i$, $J_{ji}(\vec{x})$ is total number of photons emitted from the unit volume at the position $\vec{x}$ per second, $G(\lambda, \vec{x})$ is the geometrical detection efficiency of the optical system for the photon of wavelength λ emitted from position $\vec{x}$, and $F(\lambda)$ is the sensitivity of the detector. Integration is taken over the whole volume of the collision chamber. In the present measurement, only a very small volume at the position $\vec{x}_0$ was limited for observation with a quartz lens. The polarization of light is negligible in a high energy region, so that the emission of photons might be taken as isotropic[4]. Therefore, $G(\lambda, \vec{x})$ is approximated to be

$$G(\lambda, \vec{x}) = \omega(\vec{x})\, T_\lambda(\vec{x})\, \delta^3(\vec{x} - \vec{x}_0)\,, \tag{16}$$

where $\omega(\vec{x})$ is the solid angle of the detection and $T_\lambda(\vec{x})$ is the transmission probability of the photons emitted from the position $\vec{x}$.
With this approximation, R_λ is related to J_{ji} as

$$R_\lambda = F(\lambda)\,\omega(\vec{x}_0)\, T_\lambda(\vec{x}_0)\, J_{ji}(\vec{x}_0)\,. \tag{17}$$

In cases I), (II) and III), J_{ji} is related to the apparent excitation cross section Q_j' as

$$J_{ji} = N_j A_{ji} = \frac{A_{ji}}{A_j} \rho\phi Q_j' \,. \tag{18}$$

Finally, from Eqs (17) and (18), we obtain the relation between the observed quantity R_λ and the apparent excitation cross section Q_j'.

$$R_\lambda = F(\lambda)\,\omega(\vec{x}_0)\,T_\lambda(\vec{x}_0)\frac{A_{ji}}{A_j}\rho\phi Q_j' \,. \tag{19}$$

4. Results and Discussions

In Fig. 4 is shown the spectrum which was produced by 145 keV proton incident on a helium gas target at the pressure 1×10^{-1}Torr.

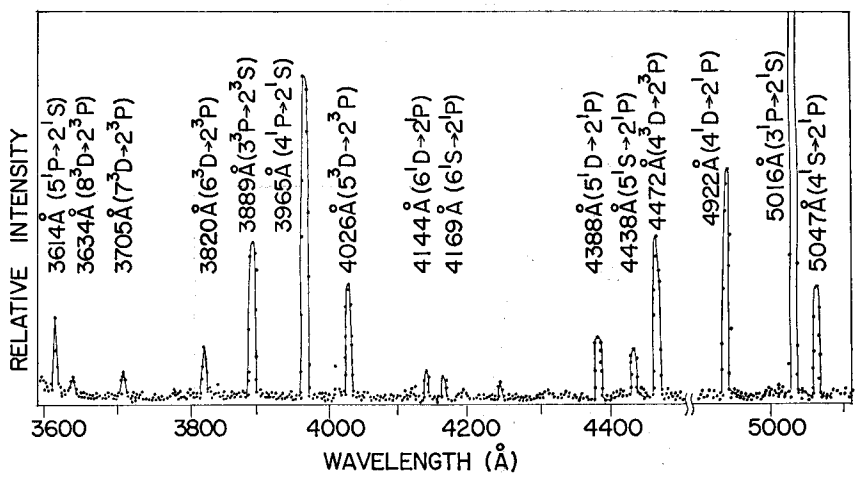

Fig. 4. Spectrum produced by 145 keV proton impact on He at 1×10^{-1}Torr.

Apparent excitation cross sections of 3^1P and 4^1P are shown in Fig. 5, which were obtained by measuring the lines 5016 Å ($3^1P\rightarrow2^1S$) and 3965 Å ($4^1P\rightarrow2^1S$), respectively. Sensitivity $F(\lambda)$ and the geometrical detection efficiency of the optical system in Eq. (19) were determined so as to make the experimental excitation cross section Q_j to be equal to that calculated with the Born approximation at 100 keV. (See the later description on the normalization of the excitation cross section of the 3^1P state). As expected from the consideration in section 3, these lines are greatly enhanced by the effect of the imprisonment of the resonance radiations of 537 Å ($3^1P\rightarrow1^1S$) and of 522 Å ($4^1P\rightarrow1^1S$), respectively. The effective chamber radius r (cm) for resonance radiation was determined as follows. The excitation cross sections $Q(3^1P)$ calculated with Eq. (7) for various r and for

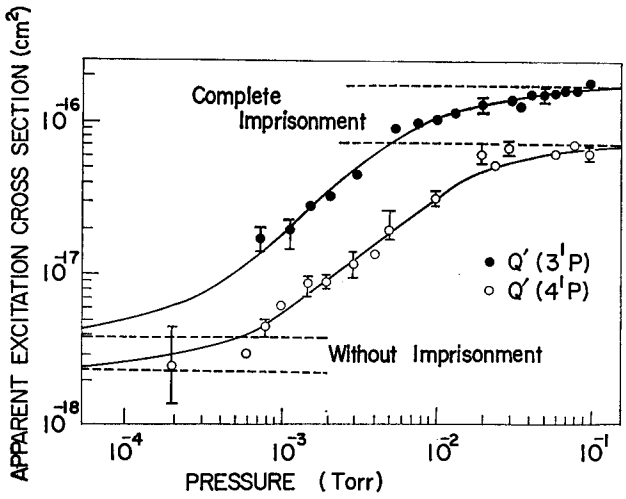

Fig. 5. Apparaent excitation cross sections of 3^1P and 4^1P of He as a function of the gas pressure by the 145 keV and 140 keV proton impact, respectively. Solid lines are calculated ones.

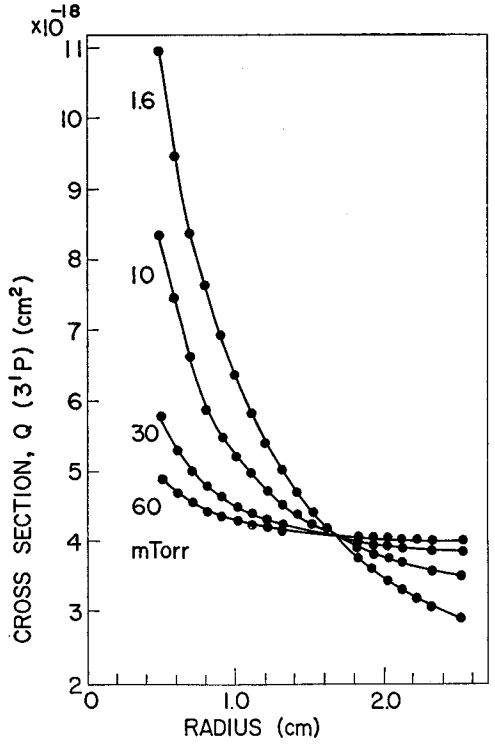

Fig. 6. Determination of the effective collision chamber radius for the imprisonment of resonance radiation 537 Å ($3^1P \rightarrow 1^1S$).

various pressures were plotted in Fig. 6. The cross section Q_j must be constant and independent of gas pressure, so that the crossing point in Fig. 6 gives the effective chamber radius (r=1.66 cm) and the correct value for the cross section ($Q(3^1P)=4.1\times10^{-18}cm^2$). The upper solid line in Fig. 5 is the calculated apparent cross section $Q'(3^1P)$ by using these values. The two dash lines in the same figure are the apparent excitation cross sections calculated with complete imprisonment ($g_j=0$) and without imprisonment ($g_j=1$), respectively. Calculation of $Q'(4^1P)$ was also made by using the same value r as that of 3^1P, and is shown by the lower solid line in the figure. It was found that the theory of imprisonment reproduces very well the experimental pressure dependence of the excitation cross sections.

In Fig. 7 is shown the excitation cross section of the 3^1P state as a function of incident proton energy. The experimental cross section of this state is normalized to the theoretical value calculated with the Born approximation at 100 keV[10]. This normalization factor is also used for other states. The energy dependence of $Q(3^1P)$ is in good agreement with that of the Born approximation. Following the calculation with the Born approximation, it is predicted that the excitation cross section of the state with the principal quantum number n is proportional to n^{-3}. In the present case, $Q(4^1P)/Q(3^1P)=0.60$ at the incident enregy 145 keV is not much different from the calculated value $(4/3)^{-3}=0.42$.

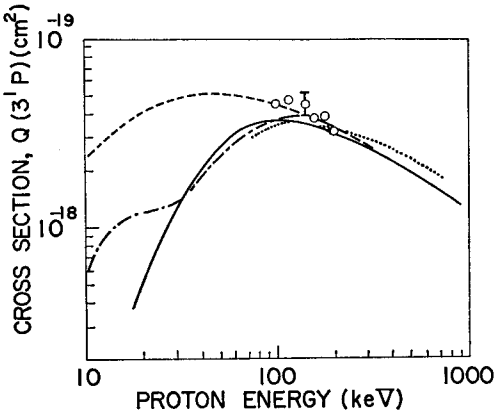

Fig. 7. Excitation cross sections of 3^1P state are compared with other experimental and theoretical values.
○ present, — • — Van den Bos[6] (exp.), ····· Thomas et al[4] (exp.) – – – Born approximation[10] (theory), —— Van den Bos[14] (theory).

In Fig. 8 are shown apparent excitation cross sections of 4^1S, 4^1D, 3^3P and 4^3D levels obtained by measuring the light intensities of 5047 Å ($4^1S\rightarrow2^1P$), 4922 Å

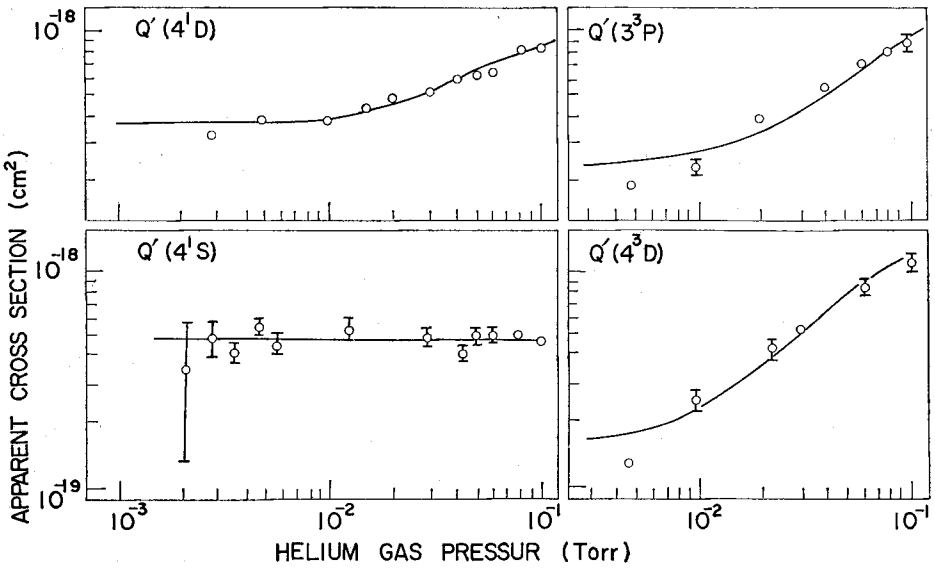

Fig. 8. Apparent excitation cross sections of 4^1D, 4^1S, 3^3P and 4^3D levels as a function of the gas pressure by the impact of 145 keV protons on He.

($4^1D \rightarrow 2^1P$), 3889 Å ($3^3P \rightarrow 2^3S$) and 4472 Å ($4^3D \rightarrow 2^3P$), respectively. The cross section $Q'(4^1S)$ seems to be constant over the whole range of the investigated pressure. Together with the pressure independence of $Q(3^1S)$ reported by Krause et al.[7], it may be concluded that the excitation of the ^1S state of helium is mainly caused by the direct proton collision mechanism. This conclusion was confirmed by the measurement of the lateral distribution of light source as shown shortly.

The apparent cross sections $Q'(3^3P)$, $Q'(4^1D)$ and $Q'(4^3D)$ show the pressure dependence, from which the collisional transfer cross sections $Q^c(3^1P \rightarrow 3^3P)$, $Q^c(4^1P \rightarrow 4^1D)$ and $Q^c(4^1P \rightarrow 4^3D)$ can be estimated by using Eq. (11). These results are tabulated in Table I. The solid lines in Fig. 8 for these states are the calculated values, using Eq. (11) with the above Q^c values. Reproducibility of the experimental pressure dependences are satisfactorily good.

Table I. Collisional transfer cross sections.

unit: 10^{-15} cm²

TRANSFER	PERSENT	REF. 1)	REF. 15)
$3^1P \rightarrow 3^3P$	5.53	12.0	
$4^1P \rightarrow 4^1D$	4.86	56.7	12.3
$4^1P \rightarrow 4^3D$	10.2	42.3	2.6
	145 keV H^+	200 keV H^+	electron

These pressure dependences are compared with those of the electron impact experiment by Heddle and Lucas[11], shown in Fig. 9. In the electron impact excitation, $Q'(4^1S)$ and $Q'(4^3D)$ begin to depart from the constant value (normalized to unity) even at a low gas pressure. The cause of this disagreement is not clear in the present study. In contrast to this, $Q'(4^1D)$ and $Q'(3^3P)$ have a fairly good agreement between the proton impact and the electron impact.

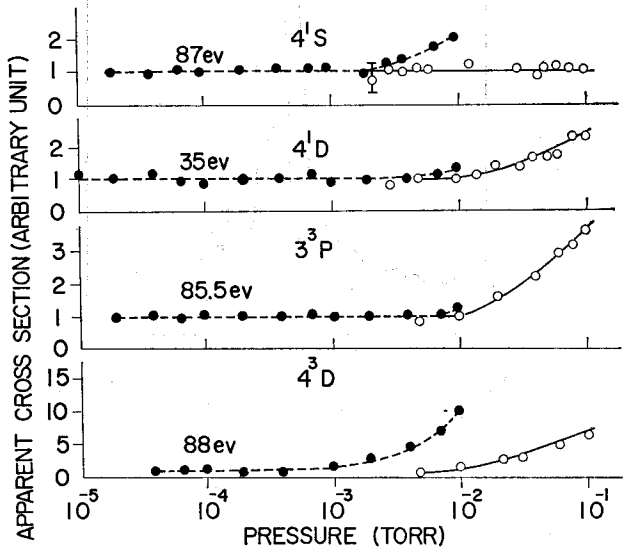

Fig. 9. Comparison of relative apparent excitation cross sections of He excited by 145 keV proton impact (○ present) with those by Heddle and Lucas[11] (eleetron impact ●).

The lateral distributions of the light sources of 5016 Å ($3^1P \rightarrow 2^1S$) and 5047 Å ($4^1S \rightarrow 2^1P$) were measured for 150 keV proton impact on helium gas at 5×10^{-2} Torr. The beam diameter is 2 mm, and the lateral observation width is limited to 2 mm by using a Hartmann slit. The results are shown in Fig. 10 where each of the maximum intensities is taken to be 100 precent. The distribution of 5047 Å light source is sharp in comparison with that of 5016 Å, and is confined almost within the beam dimaeter. This result and the pressure independence of $Q'(4^1S)$ indicate the direct excitation mechanism of the 4^1S state. Broadening of the lateral distribution may be expected for line 5016 Å since the excitation of the 3^1P state at 5×10^{-2}Torr is greatly influenced by the effect of imprisonment. The relation between the broadening and the effective chamber radius r is not clear at the present stage.

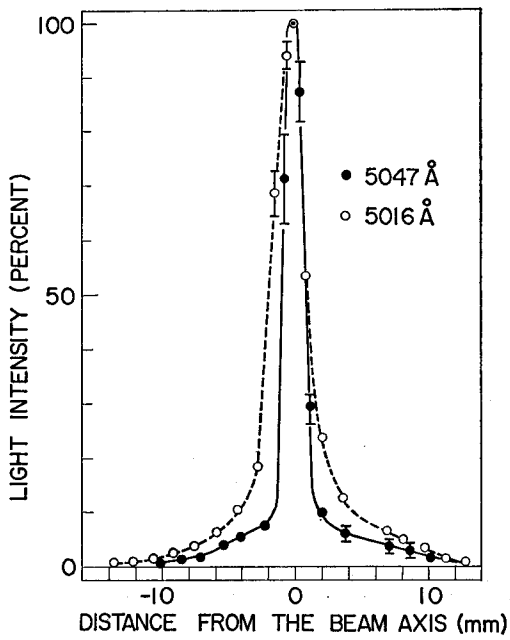

Fig. 10. Light intensities of 5016 Å ($3^1P \rightarrow 2^1S$) and 5047 Å ($4^1S \rightarrow 2^1P$) as a function of the distance from the beam axis.

The excitation cross section $Q(4^1S)$ is in good agreement with the experimental data Provided by Van den Bos et al[6]., as shown in Fig. 11. The theoretical values obtained by the scaling relationship from the electron impact calculation[12] is also shown for comparison. The excitation of this state from the ground state is optically forbidden, and is expected to be a quadrupole transition. Following the Bethe-Born approximation, the cross section multiplied by the incident energy is constant for the quadrupole transition. This was confirmed by plotting $Q(4^1S)E$ as a function of E in our case.

The excitation cross sections of the 3^3P state are shown in Fig. 12 as a function of incident proton energy. There is no reported data of proton impact with which it can be compared. Energy dependence is represented as $E^{-2.6}$. In the electron impact excitation, the E^{-3} dependence is predicted by the Ochkur approximation which takes into account the electron exchange mechanism. Showalter et al.[13] reported $E^{-3.5\pm0.2}$ dependence of the excitation of this state in the electron impact experiment. In the proton impact case, however, it is not clear how far the secondary electron affects the excitation of the state. Detailed information about such processes may be obtained from the systematic measurement of the lateral distribution of the light source.

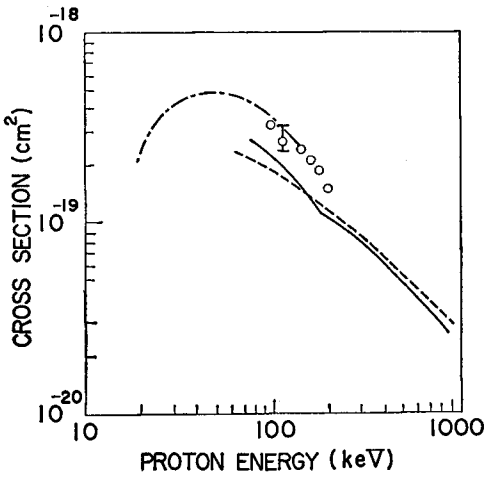

Fig. 11. Excitatin cross sections of the 4^1S state are compared with other data.
○ present, —·— Van den Bos[6] (exp.), —— Thomas et al.[4] (exp.), ····· Gaillard[12] (theory).

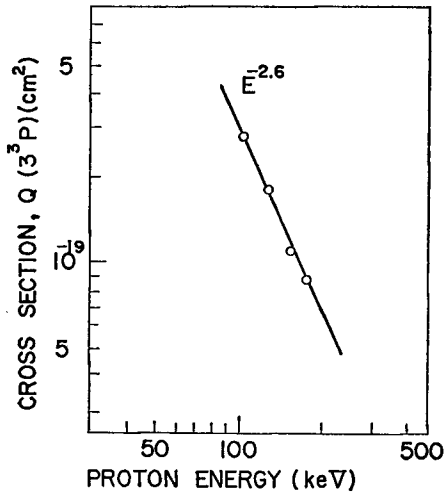

Fig. 12. Excitation cross sections of the 3^3P state.

5. Conclusions

Light intensities and their lateral distribution of line spectra from the helium gas target bombarded with 100–200 keV protons were studied. The main purpose of this work is the study of the excitation processes over a wide range of target gas pressure, in which the secondary mechanisms also play important roles. While systematic studies on these mechanisms by electron impact excitation have been made, there are very few experiments with proton and other heavy ion impact.

The pressure dependence of light intensities shows that the population of the resonance levels n^1P (n=3,4) is greatly increased by the effect of imprisonment, and that 4^1D, 4^3D and 3^3P states are influenced by the collisional transfer effects. However, the collisional transfer effect does not contribute to the 4^3D state excitation even at fairly high pressure in contrast to the case of electron impact expact experiment. The excitation of the 4^1S level is independent of target gas pressure and its lateral distribution is confined within the beam diameter. These results indicate that any secondary mechanism does not participate in the excitation of the 4^1S state.

Acknowledgements

The authors would like to express thanks to Messrs. Y. Kido, T. Ogawa and

K. Tsumaki for their assistance during the whole stage of this work. The valuable discussions with Prof. M. Sakisaka and Messrs. M. Tomita, N. Maeda, N. Kobayashi and H. Hori are also gratefully acnowledged.

References

1) R.H. Hughes, R.C. Waring and C.Y. Fan; Phys. Rev. **122**, 525 (1961).
2) J.G. Dodd and R.H. Hughes; Phys. Rev. **135**, A618 (1964).
3) J. Van Eck, F.J. De Heer and J. Kistemaker; Physica **30**, 1171 (1964).
4) E.W. Thomas and G.D. Bent; Phys. Rev. **164**, 143 (1967).
5) Daniel Krause, Jr and Edward A. Stoltysik; Phys. Rev. **175**, 142 (1968).
6) J. Van den Bos, G.J. Winter and F.J. De Heer; Physica **40**, 357 (1968).
7) Daniel Krause, Jr and Edward S. Stoltysik; Phys. Rev. A**6**, 694 (1972).
8) A. Itoh, M. Asari and F. Fukuzawa; Mem. Fac. Engng., Kyoto Univ. **39**, (1977).
9) A.H. Gabriel and D.W.O. Heddle; Proc. Roy. Soc. (London) A**258**, 124 (1960).
10) R.J. Bell; Proc. Phys. Soc. **78**, 903 (1961).
11) D.W.O. Heddle and C.B. Lucas; Pro. Roy. Soc. (London) **271**, A129 (1963).
12) M. Gaillard; Compt. Rend. **263**, 549 (1966).
13) J.G. Showalter and R.B. Kay; Phys. Rev. A**11**, 1899 (1975).
14) J. Van den Bos; Phys. Rev. **181**, 191 (1969).
15) D.T. Stewart and E. Gabathuler; Proc. Phys. Soc. (London) **74**, 473 (1959).